Accepted Manuscript

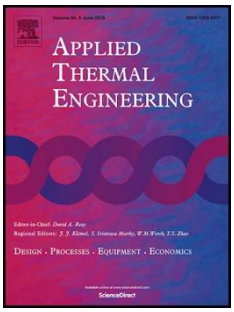

Title: Numerical study of pulverized coal-fired utility boiler over a wide range of operating conditions for in-furnace SO_2/NO_x reduction

Author: Srdjan Belošević, Ivan Tomanović, Nenad Crnomarković, Aleksandar Milićević, Dragan Tucaković

PII: S1359-4311(15)01242-9
DOI: http://dx.doi.org/doi: 10.1016/j.applthermaleng.2015.10.162
Reference: ATE 7287

To appear in: *Applied Thermal Engineering*

Received date: 23-6-2015
Accepted date: 31-10-2015

Please cite this article as: Srdjan Belošević, Ivan Tomanović, Nenad Crnomarković, Aleksandar Milićević, Dragan Tucaković, Numerical study of pulverized coal-fired utility boiler over a wide range of operating conditions for in-furnace SO_2/NO_x reduction, *Applied Thermal Engineering* (2015), http://dx.doi.org/doi: 10.1016/j.applthermaleng.2015.10.162.

Numerical study of pulverized coal-fired utility boiler over a wide range of operating conditions for in-furnace SO_2/NO_x reduction

Srdjan Belošević[a], Ivan Tomanović[a], Nenad Crnomarković[a], Aleksandar Milićević[a], and Dragan Tucaković[b]

[a]**University of Belgrade, Vinča Institute of Nuclear Sciences, Laboratory for Thermal Engineering and Energy**, PO Box 522, 11001 Belgrade, Serbia

[b] **University of Belgrade, Faculty of Mechanical Engineering**, Kraljice Marije 16, 11120 Belgrade 35, Serbia

Corresponding author: Srdjan Belošević, v1belose@vinca.rs, PO Box 522, 11001 Belgrade, Serbia, +381 11 3408-834

Highlights

1. FSI de-SO_2 and combustion modifications for de-NO_x studied by in-house developed code

2. FSI efficiency increased with proper distribution of finely grinded $CaCO_3$ particles

3. Sorbent transport air injected into the furnace affected NO_x emission

4. FSI process was not disturbed under 90% and 80% of the boiler full-load conditions

5. Increase in FGR decreased NO_x, but also boiler efficiency and SO_2 reduction

Abstract: Important tasks during pulverized coal-fired utility boilers exploitation are efficient utilization of variable quality fuels, operation in a wide range of loads and emission reduction of pollutants, like oxides of nitrogen and sulfur. Combustion process modifications for NO_x control and the furnace sorbent injection for SO_2 control are cost-effective clean coal technologies. For optimization of boiler operation mathematical prediction is regularly used and the need for modeling is most apparent in complex flows, such as turbulent reactive flows in coal-fired furnaces. Simulation of processes in a utility boiler pulverized lignite-fired furnace was performed by an in-house developed numerical code. The code is a promising numerical tool to be used also by engineering staff dealing with the process analysis in boiler units. A broad range of operating conditions was examined, such as different boiler loads, fuel and preheated air distribution over the burners and the burner tiers, grinding fineness of coal, cold air ingress and recirculation of flue gases from the boiler exit. Ash deposit on the screen walls, affecting the heat exchange inside the furnace, was considered as well. Simulations suggested optimal combustion modifications providing NO_x emission reduction, with the flame geometry improvement, as well. SO_2 reduction by injection of pulverized Ca-based sorbents into the furnace was also analyzed. Models of the sorbent particles calcination, sintering and sulfation reactions were optimized and implemented within the numerical code. Numerical experiments considered different operation parameters, such as Ca/S molar ratio, sorbent particles size and dispersion, local gas temperature in different injection zones and the particles residence time. A proper distribution of finely grinded sorbent particles could be expected to provide an efficient absorption of SO_2. With respect to the boiler thermal calculations, the facility should be controlled within narrow limits of operation parameters, due to often contradictory requirements with respect to emission reduction and the boiler unit efficiency with safe operation of superheaters. A number of influencing parameters requires

such a complex approach to evaluate alternative solutions and enable efficient, low emission and flexible operation of power plant boiler units.

Key words: *modeling, utility boiler, pulverized lignite, combustion modifications, Ca-based sorbents*

1 Introduction

Increase in the use of fossil fuels, like coals of different quality, can be anticipated in the forthcoming decades. Coal-fired power plant technology should provide higher efficiency of energy transformation, emission reduction of pollutants like oxides of nitrogen and sulfur and power plants flexibility, both with respect to operation in a wide range of boiler loads and efficient utilization of variable and low quality fuels. It is also important availability of the facilities in different operation regimes. Power stations need to be flexible in terms of loads, because shutdown and start-up modes are to be minimized and coal-fired power stations are to cofire biomass in order to reduce carbon dioxide emission. In analysis and process optimization mathematical models are regularly used [1-12], often in conjunction with laboratory and full-scale measurements. The models and software tools enable comprehensive and high-level analysis of boiler and furnace processes and operation. Considering limitation of emissions from large combustion plants, the Electric Power Industry of Serbia is to apply corresponding regulations of European Union, so that significant efforts are planned in improving both energy and ecology efficiency of power plant units. In order to meet the requirements for fuel range flexibility and low load operation, novel and improved combustion technologies and tools, including numerical analysis, are to be applied also for retrofit of the power plant boilers.

Oxides of nitrogen are among the most important pollutants and considerable attention has been given to the modeling of NO_x formation/destruction and prediction of NO_x emission [4-6,7,13], where NO and NO_2 are referred to as NO_x. Most authors predict production and destruction of NO only [4,6,7], since it is most abundant NO_x compound in flue gases from coal combustion. In most NO simulations, prompt NO is neglected, while thermal NO and fuel NO are considered [4-6]. The most significant is fuel NO (typically accounts for 75-95% of total NO), while thermal NO becomes significant only at higher flame temperatures,

greater than 1600 K-1800 K [13]. Prompt NO is important only in extremely fuel-rich flames, so it is neglected also in the present model. Primary measures for NO_x control (combustion modifications) offer a cost effective means of NO_x emission reduction (up to 60%) [13], whereas secondary measures based on the flue gas post-combustion clean-up, are considerably more expensive. In numerical simulations of NO_x reduction done by other authors different furnace shapes and sizes can be seen [4-7]. Authors mostly tried to verify some of the primary methods for NO_x reduction and to optimize the combustion process. Multiple stage combustion showed good NO_x reduction [4-6], while influence of burner modifications on NO_x reduction was considered in some studies [4].

Emission of SO_2 from power plants and acid rains are important ecological problems. The European directives set serious SO_2 emission limits, so new technologies and facilities modernizations are necessary. Wet scrubbers are the most commonly used de-SO_2 technique, offering more than 95% of reduction efficiency; however, they have high capital and exploitation costs. Although dry sorbent injection is not a new method, it offers a promising, low capital costs, low-water, retrofitable alternative technology, compared with spray drying and wet scrubbing. Furnace sorbent injection (FSI), most commonly applies calcium-based sorbents, having relatively high reactivity and causing manageable deposits. Efficiency of this technique is up to 40%, or higher; staged FSI can lead to increase in SO_2 removal efficiency to 85%, with possibility of coupling with NO_x air-staging. FSI is best suited to boilers with lower power output, shorter life cycles and moderate SO_2 control and may be a competitive technology, standalone or in combination, especially for combustion of coals with relatively low-sulfur content. The SO_2 removal process by FSI depends on a number of parameters [14], such as sorbent type, particle size and calcine surface area, injection temperature, temperature-time history, initial SO_2 level [3]. Critical to the success of the FSI application is the ability to achieve fast and uniform dispersion and mixing between sorbent and combustion

products, during the sorbent residence time within the reaction temperature window of approximately 1000°C-1300°C, without sorbent deactivation due to sintering [3,14,15]. These processes influence the sorbent utilization, the SO_2 capture efficiency and the costs. The most reactive sorbents, like hydrated lime, are finely grinded, with mass mean diameter up to 10 μm [3]. Between energy costs to produce fine particles and increased sorbent utilization may exists a trade-off [14]. Potential impacts on power plant operation and reliability are as crucial in applicability of the technology as SO_2 removal efficiency [15]. Because deposits from FSI are more friable and have lower tube-to-deposit bonding strenght than deposits of coal ash, the sorbent-ash deposits can be treated simply by more frequent use of standard sootblowers [15]. Various modeling approaches can be used to describe the desulfurization reactions between the sorbent particles and the flue gases, such as unreacted shrinking core models, grain models and pore models [16]. In this work, different models were selected depending on the sorbent particles sizes: for particles of about 10 μm in diameter, a partially sintered spheres model (PSSM) of the limestone sulfation (belonging to the grain-class of models), in conjunction with adequate models of calcination and sintering and Borgwardt's semi-empirical unreacted shrinking core model of the lime sulfation for particles diameter of the order of magnitude 100 μm.

In this numerical study, FSI and different combustion modifications were investigated in Kostolac-B 350 MW_e boiler tangentially-fired furnace, affecting the SO_2 and NO_x emissions as well as the operation of the boiler utilizing pulverized Serbian lignite. Due to the complexity and interactions of processes, emphasis was given to the examination of a wide range of operating conditions, such as fuel and air distribution over the burners, grinding fineness of coal, cold air ingress, flues gases recirculation from the boiler exit and different boiler loads. Numerical experiments on the FSI itself considered a number of parameters, like Ca/S molar ratio, sorbent particles size and dispersion, as well as flue gas temperature and

location of the sorbent injection zones for injection above the burners, through the fuel feeding line and in combination. Attention was also paid to simultaneous effects of de-SO_2 by FSI and perspective de-NO_x primary measures. Because FSI and combustion modifications affect the boiler operation and efficiency, thermal calculations were done to avoid the boiler unit efficiency decrease and to assure required superheated steam temperature.

Analysis of the furnace processes was done by a 3D differential comprehensive combustion model and numerical code describing also NO_x formation/destruction reactions, developed in-house, previously validated against available large-scale measurements of temperature and the emissions and applied for parametric analysis and the flame and emission control [8-12]. The model is also coupled with selected and optimized submodels of $CaCO_3$ sorbent calcination, sintering and sulfation to describe the FSI process. The software is designed to be used also by engineering staff working at the power plants. Variation of operation parameters in the case-study furnace is facilitated by a special user-friendly interface [8-10], complying with the efforts to make CFD modeling capabilities accessible to non-experts, that can reduce the time to set up simulations [1]. Application of the developed software makes it possible to increase the boiler efficiency, reduce the coal consumption and decrease losses and the emission, with considerable cost savings.

2 Mathematical model and computer code

In-house developed comprehensive combustion model of processes in pulverized coal-fired furnace at stationary conditions is fully described in [8-12], coupled with submodels of NO_x formation/destruction and Ca-based sorbent reactions. User-friendly interface for data input is built within the code, with the sorbent injection panel also added [8].

Two-phase flow is modeled by Eulerian-Lagrangian approach. Gas phase is described by time-averaged Eulerian conservation equations for mass, momentum, energy, gas mixture

components concentrations, turbulence kinetic energy and its rate of dissipation. In general-index notation:

$$\frac{\partial}{\partial x_j}\left(\rho U_j \Phi\right) = \frac{\partial}{\partial x_j}\left(\Gamma_\Phi \frac{\partial \Phi}{\partial x_j}\right) + S_\Phi + S_p^\Phi \tag{1}$$

with additional sources due to particles $S_p^{\square}$, while $\square$, U_j, $\square_{\square}$ and $S_{\square}$ are gas-phase density (kg/m^3), velocity components (m/s), transport coefficient and source term for general variable $\square$, respectively; k-$\square$turbulence model is used to close the equations (1). The dispersed phase is described by differential equations of motion, energy and mass change in Lagrangian field. Particles-to gas impact is considered by PSI Cell method. Convective-radiative heat transfer is considered and the radiative exchange is modeled by the six-flux method. Calculation procedure for prediction of the furnace walls ash deposits impact on the radiative heat exchange was also developed [17] and incorporated within the comprehensive code. Experimental data for particle kinetics of Serbian lignites [10,11] with respect to the entire coal particle was used, i.e. individual phenomena in combustion were treated together. Combustion of coal particle is modeled with respect to the "shrinking core" concept of char combustion. Mass and heat addition in the equations (1) due to combustion is considered by the sources due to particles. Discretization of partial differential equations is done by control volume method and hybrid-differencing scheme and discretized equations are solved by SIPSOL method. Continuity and momentum equations are coupled by SIMPLE algorithm. The code was verified by the grid-independence study, with numerical error assessment [11]. For prediction of thermal NO simplified Zeldovich expression is used [13]. The NO_x submodel comprises also the reactions of fuel NO formation and depletion [18,19], in the first place through hydrogen cyanide (HCN) originating from volatilization. The chosen model is in conjunction with De Soete global-reaction kinetics for the gas-phase NO formation [19]. The fuel NO formation reaction rate depends on gas temperature and concentrations of

oxygen and HCN. For NO depletion rate the expression is selected according to [18], as a function of mole fractions: X_{HCN}, X_{O2}, X_{NO}. Transport equations (2) for NO and HCN are solved in Eulerian field. The source of NO, S_{NO}, is obtained in dependence on the total net formation/destruction rate of NO, while the source of HCN, S_{HCN}, comprises both the HCN release by devolatilization and HCN depletion. Mass fractions of NO and HCN are given by X_{NO} (kg/kg) and X_{HCN} (kg/kg), while $\square_{NO}$ and $\square_{HCN}$ are corresponding transport coefficients.

$$\frac{\partial}{\partial x_j}\left(\rho U_j X_{NO}\right) = \frac{\partial}{\partial x_j}\left(\Gamma_{NO}\frac{\partial X_{NO}}{\partial x_j}\right) + S_{NO},$$

$$\frac{\partial}{\partial x_j}\left(\rho U_j X_{HCN}\right) = \frac{\partial}{\partial x_j}\left(\Gamma_{HCN}\frac{\partial X_{HCN}}{\partial x_j}\right) + S_{HCN} \quad (2)$$

The NO_x formation/destruction submodel is described in details and validated by comparisons with the available emission measurements on the case-study boiler units [9].

Injection of limestone ($CaCO_3$) sorbent particles into the furnace brings about the reactions of calcination, sintering and sulfation [20]. Calcination, i.e. endothermic decomposition of $CaCO_3$ to lime (CaO) and CO_2: $CaCO_3$ □ CaO + CO_2 takes place very fast, resulting in significant increase of porosity of CaO particle. Due to the particle heating below its melting point, sintering (i.e. fusion of particle pores) occurs [21]. Increased temperatures (900°C-1100°C and above) favor this mechanism [22]. Due to the reduction of porosity and the effective surface of the particle, sintering negatively affects exothermic sulfation (absorption) reaction: CaO + SO_2 + □ O_2 □ $CaSO_4$.

One approach to model these processes, Borgwardt's semi-empirical unreacted shrinking core model of the lime sulfation (implicitly taking into account also the sintering) [23] was selected for relatively large particle sizes (e.g. with diameter of about 100 μm) [8]. SO_2 and O_2 reach the porous surface of CaO and react to produce calcium-sulphate ($CaSO_4$) which fills the pores of lime, forming the so-called "product layer" [22]. The reaction rate is first

controlled by kinetics and later by diffusion through the layer; the sulfation is slowing, ending when SO_2 and O_2 are no longer able to diffuse. An unreacted CaO core remains, surrounded by $CaSO_4$. The model based on this kind of approach had been validated [24] against experimental data [23]. It was also described and implemented in [8,25]. Detailed analysis of the numerical results showed, as expected, that relatively large particles were not nearly utilized to their full potential. In this work, the sorbent particles of 10 μm in diameter were considered, but for this size class different modeling approaches appear to be by far more appropriate, while the Borgwardt's model relies on simplified kinetics measured for limestone particles of 70-100 μm. Several models of the sorbent particle reactions with SO_2 are available [26]. A partially sintered spheres model (PSSM) of the limestone sulfation, presented by Lindner [27], and by Alvfors [28], was selected, combined with models of particle calcination and sintering introduced by Alvfors [28,29]. Comparative analysis of Borgwardt's semi-empirical and PSS model of sulfation shows their advantages and limitations [30].

For PSS model of sulfation (absorption of SO_2), the sorbent particle reaction surface involved in the sulfation is determined by modeling of the calcination and the sintering. The total surface area of calcium sorbent consists of $CaCO_3$ part S_{CaCO3} (m^2/g) and CaO part S^n_{CaO} (m^2/g), depending on the extent of calcination $X_c(t)$, at a given time step. Loss of the surface due to sintering of the particle is also modeled [29,31], assuming that the particle consists of spherical grains connected by necks; during the sintering, the necks begin to overlap. At a given time step, the surface area of CaO part of the particle is obtained by the equation (3):

$$S^{n}_{\mathrm{CaO}} = \sum_{k=1}^{n} S_{0,\mathrm{CaO}}\left(1-\left(K_s(T_k)t_n\right)^{1/\gamma(T_k)}\right)\left(X_c(t_k)-X_c(t_{k-1})\right) \tag{3}$$

$S_{0,CaO}$ (m^2/g) is the nascent calcium surface area [21], K_s (1/s) is the sintering rate kinetic factor and □is the sintering coefficient. $S^n_{0,Ca}$ (m^2/cm^3) is the total surface area of calcium in

the particle at the time step n and it can be determined by the equation (4); M_M (g/mol) and V_M (cm^3/mol) are molar mass and molar volume of components and ε_{Ca} is the particle porosity:

$$S_{0,\mathrm{Ca}}^{n} = \frac{(X_c(t_n)S_{\mathrm{CaO}}^{n}M_{M,\mathrm{CaO}} + (1-X_c(t_n))S_{\mathrm{CaCO_3}}M_{M,\mathrm{CaCO_3}})}{X_c(t_n)V_{M,\mathrm{CaO}} + (1-X_c(t_n))V_{M,\mathrm{CaCO_3}}}(1-\varepsilon_{\mathrm{Ca}}) \tag{4}$$

The simplified PSS model [31] of sulfation accounts for complex geometry of the sorbent particle, assuming that it consists of small non-porous spherical grains in contact with each other [29]. Reaction rate of the particle is obtained when interaction of local kinetics and pore diffusion is solved from the equation (5), while local reaction rate is determined from the equation (6):

$$\frac{1}{z^2}\frac{\mathrm{d}}{\mathrm{d}z}\left(z^2\delta\frac{\mathrm{d}C}{\mathrm{d}z}\right) = -\Phi_{\mathrm{Th}}{}^2\frac{C}{S_0/S_2 + DaLS_0/l_0S_{avg}} \tag{5}$$

$$-\bar{r} = \frac{-r_A}{kc_{A0}S_0} = \frac{C}{\frac{S_0}{S_2} + \frac{DaLS_0}{l_0S_{avg}}} \tag{6}$$

where r_A is reaction rate on the particle surface, k (m/s) is the sulfation reaction rate constant, c_{A0} (mol/m^3) is concentration of SO_2 as a reactant. The reaction rate depends on the specific surface of unreacted core of the particle S_2 (m^2/m^3), the initial specific surface of the particle S_0 (m^2/m^3) and the specific surface of the product layer S_1 (m^2/m^3), which ca be determined by the equation (7). Φ_{Th} presents the Thiele modulus, C is local concentration of reactant over z (dimensionless coordinate in the particle), Da is Damköhler number, L (m) is the product layer thickness, l_0 (m) is characteristic distance.

$$S_i = \frac{3(1-\varepsilon_0)\left(2g_i^2 - mg_i(g_i-\lambda)\right)}{r_0\left(2 - m(1-\lambda)^2\left(1+\frac{\lambda}{2}\right)\right)} \tag{7}$$

ε_0 is the initial particle porosity, g_i is dimensionless radius of a grain, m is the number of grains in contact, λ is the particle structural parameter and r_0 (m) is a single grain radius for

initial time step. When reaction begins unreacted core reduces in size and its radius changes to r_2 (dimensionless radius $g_2 = r_2/r_0$), while the product layer increases in size, having radius r_1 ($g_1 = r_1/r_0$). Change of unreacted core diameter over dimensionless time depends on the initial surface S_0 and the surface of unreacted core S_2 and on the reaction rate, equation (8), while the change of the product layer diameter is determined from volumetric balance, equation (9), which depends on extent of sulfation at a time step X_s(t), equation (10) and g_2, equation (8).

$$\frac{\mathrm{d}g_2}{\mathrm{d}t^*} = \frac{S_0}{S_2}\bar{r} \tag{8}$$

$$g_1^3 - g_2^3 - \frac{m}{4}\left((g_1-\lambda)^2(2g_1+\lambda) - F(g_2,\lambda)\right) = \alpha X_s\left(1 - \frac{m}{4}(1-\lambda)^2(2+\lambda)\right) \tag{9}$$

$$X_s = 1 - \frac{g_2^3 - \frac{m}{4}F(g_2,\lambda)}{1 - \frac{m}{4}(1-\lambda)^2(2+\lambda)} \tag{10}$$

$F(g_2,\square)$ is structural function depending on extent of particle sulfation, $\square$is molar volume ratio.

The model is explained in more details in [27-31]. It was validated in conjunction with numerically simulated model of drop down tube reactor [31] by comparisons with available experimental data [32] and applied for simulation of Ca-based sorbent reactions under pulverized coal combustion conditions [33]. Initial particle parameters are used with respect to the experimental data [29,32].

Transport equation for SO_2 component of gas mixture has two source terms due to particles, from combustion of coal and due to absorption of SO_2 by CaO:

$$\frac{\partial}{\partial x_j}\left(\rho U_j X_{\mathrm{SO_2}}\right) = \frac{\partial}{\partial x_j}\left(\Gamma_{\mathrm{SO_2}} \cdot \frac{\partial X_{\mathrm{SO_2}}}{\partial x_j}\right) + S^{m}_{\mathrm{p,SO_2}} + S^{\mathrm{CaO}}_{\mathrm{p,SO_2}} \tag{11}$$

while Γ_{SO2} is transport coefficient for SO_2 and X_{SO2} (kg/kg) is SO_2 mass fraction.

3 Results and discussion

The comprehensive 3D combustion code, in conjunction with submodels of the NO_x formation/depletion and the FSI process and related reactions, was used to investigate the impact of a number of parameters in the case-study boiler furnace. Predictions of SO_2 release from coal and the NO_x emission were validated against available field measurements [8] and [9], respectively. Grid independence study suggested using 3D staggered structured mesh having 549250 nodes in total, in conjunction with 800 coal particle trajectories per burner, to achieve convergence, accuracy and calculation efficiency [11]. Regarding the sieve analysis, Rosin-Rammler distribution of particle size classes and repeated numerical experiments, representative initial mean diameter d_p=150 μm of monodispersed pulverized coal was selected.

The case-study Kostolac B1 and B2 utility boiler units (nominal steam capacity 1000 t/h and power output 350 MW_e at full load, each) are of tower-type with natural circulation [34]. Each unit has one identical water-wall dry-bottom furnace (dimensions: 15.1 m x 15.1 m x 43.0 m), with after combustion device. The furnace, burning pulverized Serbian lignite Drmno, is tangentially fired by eight jet burners, with four tiers each: two lower-stage burners (the main burners, for combustion of larger particle size classes) and two upper-stage burners. In nominal regime, seven burners are in operation, the guarantee coal lower heating value (LHV), as received: 7327 kJ/kg, total/combustible sulfur content, as received: 1.16%/0.64%, while the pulverized coal moisture content: 8.83%; coal through lower-stage burners (lower/upper tier): 45.5/24.5%, coal through upper-stage burners (lower/upper tier): 19.5/10.5 %, secondary air through the lower-stage burners: 68%. Numerical investigations of de-SO_2 by FSI and de-NO_x by combustion modifications were performed not only with respect to the nominal operating conditions, but also for the measured test-cases with the fuel having LHV,

as received: 8226 kJ/kg and 8463 kJ/kg. Operating conditions for the nominal working regime and the measured test-cases, with the arrangement of the burners are presented in details [9].

3.1 Impact of the FSI process parameters on the SO_2/NO_x emission and the case-study boiler unit operation

For direct injection of $CaCO_3$ sorbent particles into the case-study furnace a number of process parameters were examined through numerical experiments. For 17 test-cases (TCs) the reference one (TC1) relates to the nominal operation regime: FEGT = 1029 °C, NO_x emission = 426.8 mg/Nm3, average SO_2 content at the furnace exit = 6816 mg/Nm3 (normal conditions: 0 °C, 1013 mbar, dry basis, 6% O_2 in flue gases). TCs FSI2-7 sorbent through the injection ports above the burners, TCs FSI8-13 sorbent through the fuel feeding line, TCs FSI14-16 combined FSI: 30%, 50% and 70% through the ports and the rest through the fuel feeding line. Ca/S ratio range was 1-3. Sorbent particle diameter was 10 μm, while in TC FSI17 it was 96 μm, for comparison. The sorbent carrying air flow was also varied (factor 1.5) with respect to the reference one (factor 1.0). Selected results are presented in Figures 1-11.

Figure 1 shows an increase of the SO_2 reduction with increase of Ca/S molar ratio, as expected. However, an excessive value of Ca/S, i.e. sorbent flow rate, is to be avoided. The sorbent carrying air flow varies with amount of sorbent injected and depends on the Ca/S molar ratio, influencing the sorbent distribution and mixing with gases. Because of the mixing process complexity, an increase of the carrying air flow provided complex influence on the SO_2 reduction. In addition, due to the longer residence time of sorbent particles within the furnace, FSI through the fuel feeding line gave better SO_2 reduction efficiency compared with the injection through the ports above the burners. Comparative presentation of the SO_2 concentration field and the sorbent particle trajectories for two test-cases (Ca/S=2.0 and

carrying air factor 1.0 in both): FSI3 (FSI above the burners, SO_2 reduction at the furnace exit 34.82%) and FSI9 (FSI through the fuel, the SO_2 reduction 41.33%) is given in Figs. 5 and 7, i.e. Figs. 6 and 8, respectively. It should be pointed out that SO_2 emissions from the boiler would be even lower than presented in the work because the predicted results relate to the SO_2 content at the furnace exit, while the absorption reactions continue also along the convective pass to some extent, depending on local gas temperatures, chemical kinetics and mixing. Dispersion of sorbent particles and mixing with flue gases within the optimum gas temperatures domain are critical to the SO_2 reduction efficiency of dry sorbent injection methods. There are often contradictory temperature requirements for sulfation and sintering reactions. In order to attain an efficient utilization of the sorbent, the particles have to be distributed with maximal residence time within the reaction temperature window of about 1100°C -1300°C, without deactivation of the sorbent due to sintering [3,14], considering variations in temperature, SO_2 and mass flux in the furnace [15]. There is strong dependence of absorption reaction on flow conditions including particles residence time. In general, longer resident time of finer sorbent particles provide better SO_2 emission reduction. In the zones above the burners residence time is typically 1-2 s, so mixing and SO_2 absorption have to take place very rapidly. Average residence times were predicted as follows: for FSI above the burners, 10 µm particles, t= 2.0 s, 50 µm particles, t= 2.5 s, while for FSI through the fuel feeding line, 10 µm particles, t= 3.5-4.0 s. In Figure 2, the SO_2 reduction is studied for combined FSI. Maximal SO_2 reduction at the furnace exit (56.18%) was predicted for 50% of the sorbent injected through the ports above the burners and the rest through the fuel feeding line (test-case FSI15, Ca/S=2.0, sorbent carrying air factor 1.0), revealing the complexity of the above mentioned dependences. The SO_2 concentration field and the sorbent trajectories (given with respect to the intensity of axial particle velocity and gas temperature) for TC FSI15 were presented in Figures 9-10.

The sorbent calcination starts at temperatures significantly below 1000 °C, while the sorbent sintering process is slow at low temperatures and becomes significant at high temperatures, usually above 1100 °C, leading to the loss of internal particle surface, previously obtained during calcination. In addition to high temperatures, the sorbent particle residence time in the high temperature zones also influences the amount of sintering that occurs, adding to the problem complexity. The sulfur released from combustion tends to stay in and around the central vortex, creating higher sulfur dioxide concentration zones in the furnace central section, with less sulfur dioxide near the furnace walls. This can be especially noticed from Figure 5. If sorbent particles are injected through the burners, Figure 8, an attempt has to be made to avoid exposing them to the highest temperatures in the vortex, but also to keep them as close as possible to the high sulfur concentration zones, Figure 6. Higher sulfur dioxide concentrations, higher reaction temperatures and longer residence time in the furnace can have a favorable influence on overall sulfur capture, even though the particles may suffer from more intensive loss of effective surface due to sintering. It can be seen from Figs. 7 b), 8 b) and 10 b), that the temperatures (given in Kelvin) do not considerably exceed optimal temperature range along the most of the sorbent particles trajectories. If this is considered, we benefit from longer particle residence times and better mixing with sulfur dioxide along with higher, but not excessive reaction temperatures, while carefully avoiding injection of majority of the sorbent particles in the very center of the flame, where they would be most certainly deactivated due to the sintering reaction.

During the FSI, apart from energy source/sink in the gas phase due to reactions, sorbent carrying air (often extracted from the combustion air) will influence the local temperature field and, consequently, not only the sorbent-to-SO_2 reactions, but also the NO_x formation/destruction process. In fuel-rich conditions SO_2 enhances the fuel NO production [35], but in the test-cases considered the fuel-lean conditions prevail, diminishing this impact,

while major effects are dependence of fuel NO on the fuel bound nitrogen and the local excess air, as well as dependence of thermal NO on local gas temperatures. Figures 3 and 4 show NO_x emission in different cases of FSI above and through the burners, respectively. Increase of the sorbent carrying air injected above the burners provided decrease of the NO_x emission, while increase of the carrying air injected through the burners (i.e. more air in the flame region and less air above the flame) provided increase of the NO_x emission.

Figure 11 presents the influence of the sorbent particle size on the SO_2 reduction in the case of FSI above the burners and for different Ca/S molar ratios. Due to a considerably better utilization of the sorbent particle finer grinding provided higher SO_2 reduction, for rest of the conditions being the same. The mean particle diameter influences the ability of sorbent to get in contact with SO_2, thus limiting the diffusion of SO_2 into the particle. This greatly reduces the particle ability to absorb SO_2 from the furnace flue gasses, especially at relatively short residence times of the sorbent particles within the furnace, characteristic for operating conditions in the pulverized coal-fired boilers. Optimal dispersion of the sorbent particles and mixing with combustion products are also strongly dependent on the particle sizes. Although grinding is energy costly process, relevant studies indicate that finer grinding might be also economically advantageous because the energy costs are often less than the savings due to the improved calcium utilization [14,15].

Since de-NO_x combustion tunings can often decrease the steam boiler efficiency, it is important to balance between the boiler efficiency and NO_x emission reduction [9]. However, impact of FSI process on the boiler efficiency is an issue that seems to be given less attention. The sorbent carrying air (i.e. transport air) lowers gas temperatures at the injection level to some extent, while slightly increased excess air can also affect the boiler efficiency [3,15]. The furnace screen walls heat absorbtion typically decreases and the convective pass heat absorption increases. In order to minimize possible negative impact of FSI on boiler thermal

performance, analysis should focus on determining the furnace gas temperature field and the boiler exchangers heat duties. For guarantee coal, the case-study boiler thermal calculations were performed with respect to predicted FEGT for the test-cases based on nominal operation regime and differing to each other by fuel and air distribution over the burners [9]. The thermal calculations suggested an optimal range of FEGT (990-1010)°C, regarding the boiler efficiency, required superheated and reheated steam temperature (540°C) and amount of water injected into the superheated and reheated steam pipeline in order to keep the temperature [8,9]. Effects of increase in the amount of water are reduced boiler efficiency and higher fuel consumption. In this study, for the most promising test-cases with respect to the de-SO_2 by FSI of 10 μm particles, FEGT was predicted as follows: for FSI above the burners: 1011°C (TC FSI4, Ca/S=3.0, sorbent transport air factor 1.0, SO_2 reduction at the furnace exit 36.91%), for FSI through the burners: 1024°C (TC FSI10, Ca/S=3.0, transport air factor 1.0, SO_2 reduction 43.79%), but also: 1010°C (TC FSI11, Ca/S =1.0, transport air factor 1.5, SO_2 reduction 31.96%),)°C and for combined FSI: 1005°C (TC FSI15, Ca/S =2.0, transport air factor 1.0, SO_2 reduction 56.18%). Maximal SO_2 reduction was predicted in TC FSI15 that could have not been expected to disturb the boiler operation.

3.2 FSI efficiency and NOx emission in different operating conditions of the case-study boiler unit

Previous numerical investigations showed that significant NO_x emission reduction could be achieved by proper modifications of combustion process, like distribution of fuel and preheated air over the burners and the burner tiers, control of local excess air and the cold air ingress, finer grinding of coal, etc., influencing also the flame position [8-10]. Complex operating conditions were also studied in this numerical study, such as different boiler loads, grinding fineness of coal, cold air ingress, recirculation of flue gases from the boiler exit and

the furnace walls ash deposits. Variations of the working parameters are expected to affect both the FSI de-SO_2 process efficiency and the boiler unit operation.

3.2.1 Grinding fineness of the case-study coal

Grinding fineness of pulverized coal was studied through the variation in initial mean particle size: d_p=50 μm and 100 μm, compared with d_p=150 μm in the reference test-case TC1. The coal and air distributions and the rest of the operating conditions were the same as in the TC1. In the FSI process, 10 μm CaCO3 particles were injected above the burners. Table 1 presents dependence of the NO_x/SO_2 emissions during the FSI, for combustion of different particle size of the coal.

A minimal decrease of NO_x emission was obtained for combustion of finer grinding of coal, but only to a certain extent (d_p=100 μm); combustion of d_p=50 μm pulverized coal gave a slight increase in the emission. For different grinding fineness different geometry of the pulverized coal flame was predicted [10]. The FSI process efficiency was increased when applied during the combustion of finer grinded pulverized coal. This might be attributed to better mixing between flue gas, finely grinded pulverized coal and small sorbent particles, providing more uniform field of combustion products, like SO_2, uniform dispersion of sorbent, and, consequently, higher SO_2 removal efficiency. However, final conclusions would require more profound analysis of the complex processes.

3.2.2 The case-study boiler load

During the utility boilers exploitation, it is important to enable wide load range over a wide fuel range, as well as a stable operation not requiring or minimizing the use of additional fuel for start-up. Low-load modes help to achieve these tasks [36]. The boiler load regime also

affects the conditions for FSI application. For example, the optimal temperature window in full-load operation is often located higher than in low-load operation [14].

Table 2 shows the SO_2 reduction efficiency by FSI in conjunction with FEGT and the NO_x emission under different loads of the case-study boiler unit. Test-cases 3 and 10 differ from the reference TC1 by the coal and air distribution, as follows. Coal through lower-stage burners (lower/upper tier), TC3: 30.4/25.8% and TC10: 27.6/43.6%; coal through upper-stage burners (lower/upper tier), TC3:30.7/13.1% and TC10: 13.9/14.9%; secondary air through the lower-stage burners: 74% for both cases. The sorbent particle mean diameter was 10 μm. Compared with the full-load operation, partial load modes: 90% of the full-load and 80% of the full-load did not disturb the FSI process, providing slightly better SO_2 removal, in accordance with investigations which reported increased SO_2 reduction at reduced load due to lower injection temperature and longer residence time of sorbent particles [15]. In the case of 70% of the full-load the burners operation regime (six burners in operation) was completely different than for 90% and 80% of the full-load (seven burners in operation, as in the reference case TC1). Due to a different flow and temperature situation in the furnace, the 70% of the full-load regime provided different impact on the SO_2 removal, as well. For all the loads of the boiler considered, the FSI caused decrease of both FEGT and NO_x emission, due to the sorbent transport air injection into the furnace above the burners.

3.2.3 Impact of ash deposits on the case-study boiler unit operation

Pulverized coal ash deposit layer is formed on the furnace screen walls, reducing the heat exchange between the flame and the walls. Due to increase of the ash deposits thermal resistance, net heat transfer rates through the walls are decreased and the furnace gas-particles medium temperatures are increased. Through the layer, heat is transferred by conduction and radiation, while physical properties influencing the heat transfer are effective thermal

conductivity and emissivity of the layer fire side surface. Ash deposits from FSI also affect the boiler thermal efficiency and performance [3]. Since sorbents are usually injected above the burners, FSI will increase deposition mainly on the convective heat transfer surfaces. Deposition of wet ash/sorbent mixture in the furnace and the convective pass is important issue in sorbent injection process, although these deposits appear to be relatively soft, so that they can be removed by standard sootblowers [15]. In the respect of the effect of ash deposits on furnace and boiler operation, numerical simulations can help to optimize temperature and flow conditions within the furnace [17].

Figures 12 and 13 present predicted influence of the ash deposit thickness on the Kostolac B utility boiler unit operation, obtained for nominal operating conditions. Increased ash slagging provides reduced heat transfer to the furnace water-walls which increases FEGT, and, consequently, also the NO_x emission. The combustion products temperature increase will also increase heat transfer to the convective pass heat exchangers. The final stages of superheater and reheater receive increased amount of heat and the amount of water injected into the superheated and reheated steam pipeline is also increased. This results in higher fuel consumption and reduced boiler efficiency. The furnace slagging is accompanied also by the fouling of the heat exchangers in the convective pass. If this would be also considered in the boiler thermal calculations, for the water-walls deposit thichness of 4 mm and 10% increase of fouling, the boiler efficiency would be about 1% less than without slagging and fouling.

3.3 FSI efficiency in the conditions of flue gas recirculation for NO_x control

Flue gas recirculation (FGR) can be an effective and economical method for reducing NOx emission [37]. Flue gases are recirculated from the boiler exit into the burner region in order to lower the combustion temperature which limits NO_x (and CO) emission. When mixed with

preheated air the recirculated gases lower also the oxygen content in the combustion zone, attenuating the NO_x formation reaction. Nowadays boilers operate with FGR rates of 0-30%. Table 3 shows selected results of the numerical predictions and the boiler thermal calculations performed with respect to the variations of measured test-cases TC8226 and TC8463 (LHV=8226 kJ/kg and 8463 kJ/kg, as received) [9]. Subject of the investigation considered the effects of both the FGR method for de-NO_x and the FSI method for de-SO_2 in complex operating conditions of FGR application. In the FSI test-cases, $CaCO_3$ 10 μm sorbent particles were injected through the ports above the burners, while Ca/S ratio was 3. In addition, some of the test-cases refer to reduced cold air ingress.

The FGR from the boiler exit in nominal regime is 4.9% of total amount of boiler exit flue gases (as in TC8463 and TC8226). Test-cases TC8463-8 and TC8463-9 (4% and 8% of FGR) compared with TC8463-7 (0% of FGR) show that increase in FGR cools the furnace gases and decreases FEGT, providing also decrease in NO_x emission (23.4% for 8% of FGR), but the boiler exit gas temperature increases and the boiler efficiency decreases to some extent. Due to increased flow of flue gases through the boiler the amount of water injected in order to control the superheted and reheated steam temperatures is also increased, reducing the boiler efficiency. In the test-cases considered required temperature of superheated and reheated steam (540°C) was attained. Decreased cold air ingress into the furnace will increase FEGT and decrease exit boiler gas temperature which provides increase in the boiler efficiency coefficient. In addition, fuel with lower quality (TC8226) provided to some extent lower FEGT.

The FSI process was examined under the FGR conditions (test-cases 8463-FSI, 8463-7-FSI, 8463-8-FSI, 8463-9-FSI and 8226-FSI). Decrease of FEGT due to the sorbent transport air injection into the furnace, as well as NO_x emission reduction, can be noticed in all FSI test-cases. Moreover, SO_2 reduction at the furnace exit was affected by the FGR conditions. More

flue gases recirculated from the boiler exit gave lower SO_2 reduction efficiency, but only to some extent: TC8463-9-FSI (VFGR =8%), provided about 3% lower SO_2 reduction at the furnace exit, compared with TC8643-7 (VFGR =0%) and about 4% lower compared with TC8643 (VFGR = 4.9%; in this case also the burners operation scheme was different). In the test cases 8463-7, 8, 9, with or without FSI, 6 burners are in operation, two opposite are turned off, so the temperature and concentration fields are almost symmetrical, Figure 14. The nitric oxide content within the furnace follows the gas temperature field, but even more both the hydrogen cyanide and the oxygen concentration fields, because the fuel NO is predominant form of nitrogen oxides formed by the pulverized coal combustion.

4 Conclusions

A differential mathematical model and in-house developed, user-friendly computer code were applied for investigation of processes in 350 MW_e boiler dry-bottom furnace, tangentially fired by pulverized Serbian lignite. Models of Ca-based sorbent particles calcination, sintering and sulfation, as well as NO_x formation/depletion reactions were coupled with the code. The furnace operating conditions were simulated in a wide range, including de-SO_2 by FSI of 10 μm $CaCO_3$ particles and de-NO_x by combustion modifications, while the effect of the conditions on the case-study boiler efficiency was examined by the boiler thermal calculations.

Numerical predictions showed increase of SO_2 capture with increase of Ca/S molar ratio. FSI through the fuel feeding line gave higher de-SO_2 efficiency than injection above the burners, due to the longer residence time of sorbent particles. The sorbent transport air lowered gas temperatures to some extent and influenced the sorbent dispersion and the SO_2 reduction. The transport air injected above and through the burners provided decrease and increase of NO_x emission, respectively. Finer grinding of sorbent particles (10 μm vs. 96 μm)

provided better de-SO_2 effect, due to considerably more efficient utilization of the sorbent. Maximal SO_2 reduction (56.18% at the furnace exit) was predicted for combined FSI, with 50% of the sorbent injected through and 50% above the burners (for Ca/S=2.0). This regime were not expected to disturb the boiler operation, according to the boiler thermal calculations suggested an optimal range of FEGT regarding the boiler efficiency and the operation of superheaters and reheaters.

The FSI process efficiency increased when applied during the combustion of finer grinded pulverized coal. Partial loads of the boiler: 90% and 80% of the full-load, with seven burners in operation as in full-load conditions, did not disturb the FSI process, providing slightly better SO_2 removal. For each boiler load, FSI caused decrease of FEGT and NO_x emission, due to the sorbent transport air injection into the furnace.

Pulverized coal ash deposits, including deposits from FSI, reduce heat transfer to the furnace water-walls, increase FEGT and NO_x emission and reduce the boiler efficiency. For the water-walls deposit thickness of 4 mm and 10% increase of the convective pass heat exchangers fouling, the boiler efficiency would be about 1% less than without slagging and fouling.

FGR from the boiler exit is an effective and economical method for reducing NO_x emission. Effects of the FGR method for de-NO_x and the FSI method for de-SO_2 in complex operating conditions of FGR application were numerically studied. In the FSI test-cases, 10 μm $CaCO_3$ sorbent particles were injected above the burners, while Ca/S=3. Increase in FGR decreased FEGT and also NO_x emission (23.4% NO_x reduction for 8% of FGR), but the boiler exit gas temperature increased and the boiler efficiency decreased. Decreased cold air ingress into the furnace increased FEGT and decreased exit boiler gas temperature, providing higher efficiency of the boiler. Due to the sorbent transport air injection, FEGT and NO_x decreased. The SO_2 reduction was also affected by the FGR conditions; more flue gases recirculated

from the boiler exit gave to some extent lower SO_2 reduction: 8% of FGR provided 3% lower SO_2 reduction at the furnace exit, compared with the case without FGR.

The numerical study demonstrated the importance of comprehensive analysis of complex, mutually dependent processes in the coal-fired furnaces and boilers under a wide range of operating conditions, for the purpose of increasing the energy and ecology efficiency of the energy conversion systems. The developed computer code proved to be an efficient numerical tool for analysis of involving processes and optimization of thermal energy facilities operation. Further improvements of corresponding submodels will additionally increase the comprehensive model ability to predict the effects of variable operating conditions on the utility boilers performance and efficiency.

Acknowledgments

This work has been supported by the Republic of Serbia Ministry of Education, Science and Technological Development (project: “Increase in energy and ecology efficiency of processes in pulverized coal-fired furnace and optimization of utility steam boiler air preheater by using in-house developed software tools”, No. TR-33018).

References

[1] Chui, E. H., Gao, H., Majeski, A. J., Lee, G. K., Performance Improvement and Reduction of Emissions from Coal-Fired Utility Boilers in China, Energy for Sustainable Development, 14 (2010) 206-212.

[2] Marocco, L., Mora, A., CFD Modeling of the Dry-Sorbent-Injection Process for Flue Gas Desulfurization Using Hydrated Lime, Separation and Purification Technology, 108 (2013) 205-214.

[3] Zhou, W., Maly, P., Brooks, J., Nareddy, S., Swanson, L., Moyeda, D., Design and Test Furnace Sorbent Injection for SO_2 Removal in a Tangentially Fired Boiler, Environmental Engineering Science, 27 (2010) 337-345.

[4] Zeng, L., Li, Zh., Zhao, G., Shen, Sh., Zhang. F., Numerical Simulation of Combustion Characteristics and NO_x Emissions in a 300 MW_e Utility Boiler with Different Outer Secondary-Air Vane Angles, Energy & Fuels, 24 (2010) 5349-5358.

[5] Coelho, L. M. R., Azevedo, J. L. T., Carvalho, M. G., Application of a Global NO_x Formation Model to a Pulverized Coal Fired Boiler with Gas Reburning, *Proceedings, 4th International Conference on Technologies and Combustion for a Clean Environment*, Lisbon, Portugal, July 7-10, 1997, Paper 9.4, pp. 1/8-8/8.

[6] Xu, M., Azevedo, J. L. T., Carvalho, M. G., Modelling of the Combustion Process and NO_x Emission in a Utility Boiler, Fuel, 79 (2000) 1611-1619.

[7] Diez, L. I., Cortes, C., Pallares, J., Numerical Investigation of NO_x Emissions from a Tangentially-Fired Utility Boiler under Conventional and Overfire Air Operation, Fuel, 87 (2008) 1259-1269.

[8] Belo□evi□, S., Tomanovi□, I., Beljanski, V., Tucakovi□, D., □ivanovi□, T., Numerical Prediction of Processes for Clean and Efficient Combustion of Pulverized Coal in Power Plants, Applied Thermal Engineering, 74 (2015) 102-110.

[9] Belosevic, S., Beljanski, V., Tomanovic, I., Crnomarkovic, N., Tucakovic, D., Zivanovic, T., Numerical Analysis of NO_x Control by Combustion Modifications in Pulverized Coal Utility Boiler, Energy & Fuels, 26 (2012) 425–442.

[10] Belosevic, S., Sijercic, M., Crnomarkovic, N., Stankovic, B., Tucakovic, D., Numerical Prediction of Pulverized Coal Flame in Utility Boiler Furnaces, Energy & Fuels, 23 (2009) 5401-5412.

[11] Belosevic, S., Sijercic, M., Tucakovic, D., Crnomarkovic, N., A Numerical Study of a Utility Boiler Tangentially-Fired Furnace under Different Operating Conditions, Fuel, 87 (2008) 3331-3338.

[12] Belo□evi□, S., Sijer□i□, M., Oka, S., Tucakovi□, D., Three-Dimensional Modeling of Utility Boiler Pulverized Coal Tangentially Fired Furnace, International Journal of Heat and Mass Transfer, 49 (2006) 3371-3378.

[13] Hill, S. C., Smoot, L. D., Modeling of Nitrogen Oxides Formation and Destruction in Combustion Systems, Progress in Energy and Combustion Science, 26 (2000) 417-458.

[14] Muzio, L. J., Often, G. R., Assessment of Dry Sorbent Emission Control Technologies Part I. Fundamental Processes, Journal of the Air & Waste Management Association (formerly known as JAPCA), 37 (1987) 642-654.

[15] Often, G. R., Muzio, L. J., McElroy, M. W., Assessment of Dry Sorbent Emission Control Technologies Part II. Applications, Journal of the Air & Waste Management Association (formerly known as: JAPCA), 37 (1987) 968-980.

[16] Wang, W., Bjerle, I., Modelling of High-Temperature Desulfurization by Ca-Based Sorbents, Chemical Engineering Science, 53 (1998) 1973-1989.

[17] Crnomarkovi□, N. □., Sijer□i□, M. A., Belo□evi□, S. V., Tucakovi□, D. R.,. □ivanovic, T. V, Tomanovi□, I. D., Stojanovi□, A. D., Numerical Determination of the Impact of the Ash Deposit on the Furnace Walls to the Radiative Heat Exchange Inside the Pulverized Coal Fired Furnace, *Full Papers Proceeding of International Conference "Power Plants 2014"*, 28-31. October 2014, Zlatibor Serbia, ISBN 978-86-7877-024-1, pp. 679–690.

[18] Solomon, P. R., Colket, M. B., Evolution of Fuel Nitrogen in Coal Devolatilisation, Fuel, 57 (1978) 749-755.

[19] De Soete, G. G., Overall Reaction Rates of NO and N_2 Formation from Fuel Nitrogen, Proceedings of the Combustion Institute, 15 (1975) 1093-1102.

[20] Stanmore, B. R., Gilot, P., Review-Calcination and Carbonation of Limestone During Thermal Cycling for CO_2 Sequestration, Fuel Processing Technology, 86 (2005) 1707-1743.

[21] Borgwardt, R. H., Sintering of Nascent Calcium Oxide, Chemical Engineering Science, 44 (1989) 53-60.

[22] Cheng, J., Zhou, J., Liu, J., Zhou, Z., Huang, Z., Cao, X., Zhao, X., Cen, K., Sulfur Removal at High Temperature During Coal Combustion in Furnaces: a Review, Progress in Energy and Combustion Science, 29 (2003) 381-405.

[23] Borgwardt, R. H., Kinetics of the Reaction of SO_2 with Calcined Limestone, Environmental Science & Technology, 4 (1970) 59-63.

[24] Beljanski, V., Tomanovi□, I., Belo□evi□, S., Sijer□i□, M., Stankovi□, B., Crnomarkovi□, N., Stojanovi□, A., Sulfation Reaction Modeling of Ca-Based Sorbent, *CD-ROM*

Proceedings, *International Conference Power Plants 2012*, ISBN 978-86-7877-021-0, Zlatibor, Serbia, October 30th - November 2nd, 2012, Paper No. E2012-086, pp. 1001-1012 (http://e2012.drustvo-termicara.com/english/list-of-submitted-papers).

[25] Tomanovi□, I. D., Beljanski, V. B., Belo□evi□, S. V., Sijer□i□, M. A., Stankovi□, B. D., Crnomarkovi□, N. □., Stojanovi□, A. D., Modelling and Optimisation of Desulphurisation Process by Direct Sorbent Injection in Furnace of Pulverised Coal Utility Boiler, *CD-ROM Proceedings, International Conference Power Plants 2012*, ISBN 978-86-7877-021-0, Zlatibor, Serbia, October 30th - November 2nd, 2012, Paper No. E2012-087, pp. 1013-1024 (http://e2012.drustvo-termicara.com/english/list-of-submitted-papers).

[26] Shi, L., Liu, G., Higgins, B. S., Benson, L., Computational Modeling of Furnace Sorbent Injection for SO_2 Removal from Coal-Fired Utility Boilers, Fuel Processing Technology, 92 (2011) 372-378.

[27] Lindner, B., Simonsson, D., Comparison of Structural Models for Gas-Solid Reactions in Porous Solids Undergoing Structural Changes, Chemical Engineering Science, 36 (1981) 1519-1527.

[28] Alvfors, P., Svedberg, G., Modelling of the Sulphation of Calcined Limestone and Dolomite – a Gas-Solid Reaction with Structural Changes in the Presence of Inert Solids, Chemical Engineering Science, 43 (1988) 1183-1193.

[29] Alvfors, P., Svedberg, G., Modelling of the Simultaneous Calcination, Sintering and Sulphation of Limestone and Dolomite, Chemical Engineering Science, 47 (1992) 1903-1912.

[30] Tomanovi□, I. D., Belo□evi□, S. V., Stojanovi□, A. D., Tucakovi□, D. R., □ivanovi□, T. V., Alternative Modeling Approaches to Sulfation Reactions of Calcium Based Sorbents Injected in the Pulverized Coal Furnace, *Proceedings, 16th Symposium on Thermal Science*

and Engineering of Serbia, SIMTERM 2013, ISBN 978-86-6055-043-1, Sokobanja, Serbia, October 22nd – 25th, 2013, pp. 65-72.

[31] Tomanovi□, I., Belo□evi□, S., Mili□evi□, A., Tucakovi□, D., Modeling of Calcium-Based Sorbent Reactions with Sulfur Dioxide, Journal of the Serbian Chemical Society, 80 (2015) 549–562.

[32] Flament, P., Morgan, M., Fundamental and Technical Aspects of SO_2 Capture by Ca Based Sorbents in Pulverized Coal Combustion, Report on the S 2 – 4 Study, 1987, Ijmuiden, Holland.

[33] Tomanovi□, I., Mili□evi□, A., Stojanovi□, A., Belo□evi□, S., Tucakovi□, D., Ca-Based Sorbent Reactions Modelling for SO_2 Emission Reduction in Pulverized Coal Combustion Conditions, *Full Papers Proceeding of International Conference "Power Plants 2014"*, 28-31. October 2014, Zlatibor Serbia, ISBN 978-86-7877-024-1, pp. 704–711.

[34] Tucakovic, D., Zivanovic, T., Stevanovic, V., Belosevic, S., Galic, R., A Computer Code for the Prediction of Mill Gases and Hot Air Distribution Between Burners' Sections at the Utility Boiler, Applied Thermal Engineering, 28 (2008) 2178-2186.

[35] Hampartsoumian, E., Nimmo, W., Gibbs, B.M., Nitrogen Sulphur Interactions in Coal Flames, Fuel, 80 (2001) 887-897.

[36] Bruggemann, H., Marling, T. M., Conventional Firing Systems for Future Power Plants, *CD-ROM Proceedings, International Conference Power Plants 2012*, ISBN 978-86-7877-021-0, Zlatibor, Serbia, October 30th - November 2nd, 2012, Paper No. E2012-004, pp. 25-34 (http://e2012.drustvo-termicara.com/english/list-of-submitted-papers).

[37] McAdams, J. D., Minimize NO_x Emissions Cost-Effectively, Hydrocarbon Processing, 80 (2001) 51-58.

Figure captions:

Figure 1: Influence of Ca/S, sorbent-carrying air and sorbent injection location on the SO_2 reduction at the furnace exit

Figure 2: SO_2 reduction at the furnace exit for combined FSI

Figure 3: NO_x emission in different cases of FSI above the burners (regarding Ca/S and the sorbent carrying air)

Figure 4: NO_x emission in different cases of FSI through the burners (regarding Ca/S and the sorbent carrying air)

Figure 5: The SO_2 content in the test-case FSI3, FSI above the burners: FEGT= 1016 °C, NO_x emission=430.0 mg/Nm^3, average SO_2 content at the furnace exit=4442 mg/Nm^3

Figure 6: The SO_2 content in the test-case FSI9, FSI through the fuel feeding line: FEGT= 1018 °C, NO_x emission = 363.9 mg/Nm3, average SO_2 content at the furnace exit = 3999 mg/Nm^3

Figure 7: Selected trajectories of the sorbent particles for FSI above the burners, test-case FSI3, a) particle axial velocity and b) temperature

Figure 8: Selected trajectories of the sorbent particles for FSI through the fuel feeding line, test-case FSI9, a) particle axial velocity and b) temperature

Figure 9: The SO_2 content in the test-case FSI15, combined FSI: 50% above the burners, FEGT=1005 °C, NOx emission = 387.6 mg/Nm^3, average SO_2 content at furnace exit = 2986 mg/Nm^3

Figure 10: Selected trajectories of the sorbent particles for combined FSI: 50% above the burners, test-case FSI15, a) particle axial velocity and b) temperature

Figure 11: Influence of the sorbent particle size on the SO_2 reduction

Figure 12: Influence of the ash deposit thickness on the FEGT and the NO_x emission

Figure 13: Influence of the ash deposit thickness on the boiler unit efficiency

Figure 14: Gas temperature, oxygen, hydrogen cyanide and nitric oxide concentration fields in the furnace for 8% of FGR from the boiler exit (test-case 8463-9)

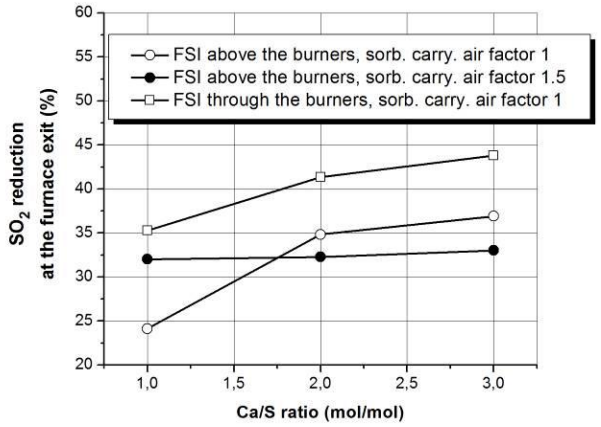

Figure 1

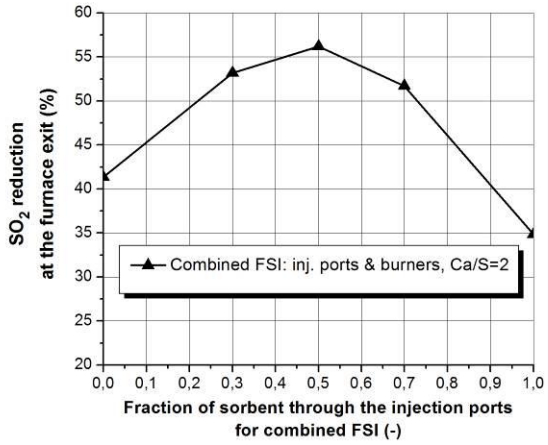

Figure 2

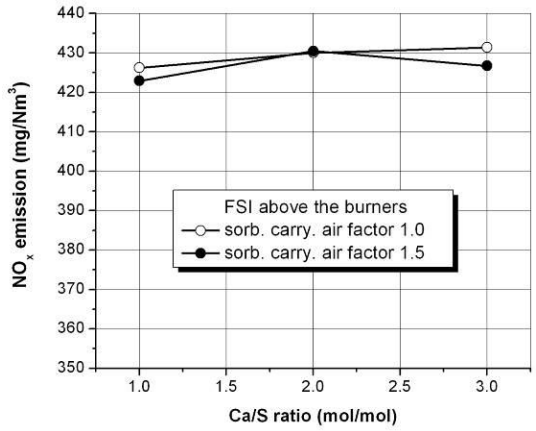

Figure 3

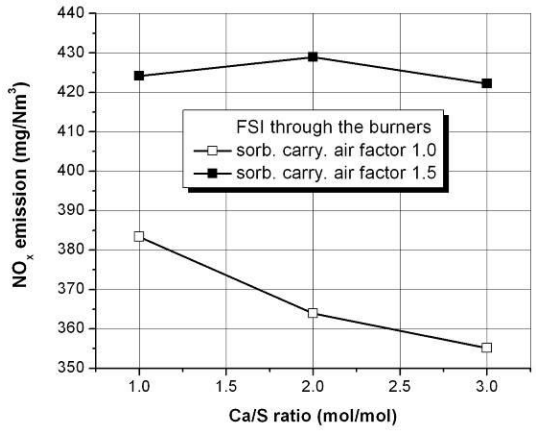

Figure 4

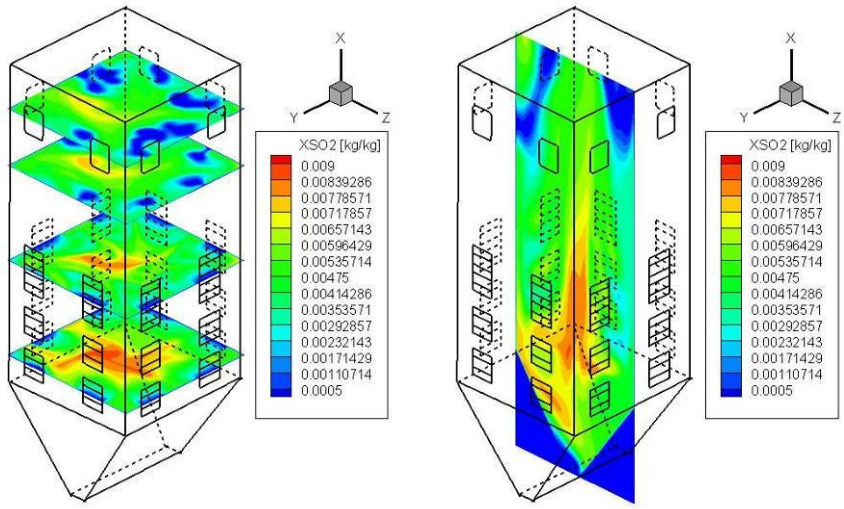

Figure 5

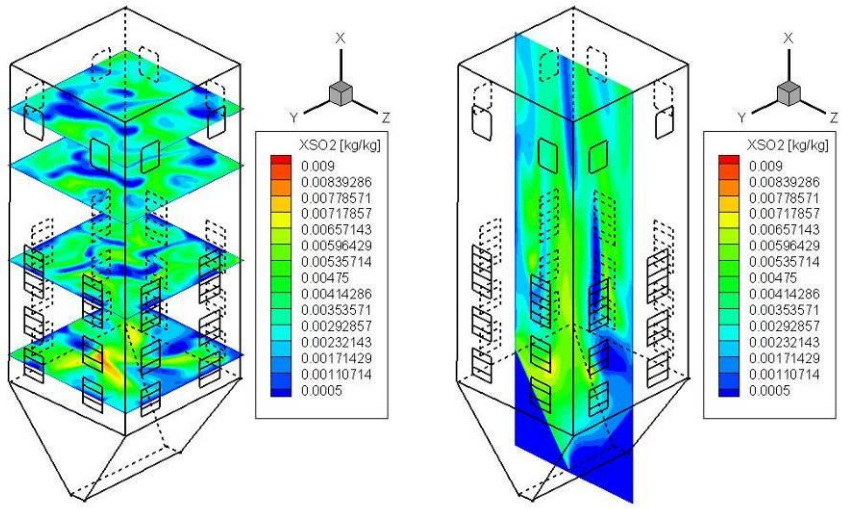

Figure 6

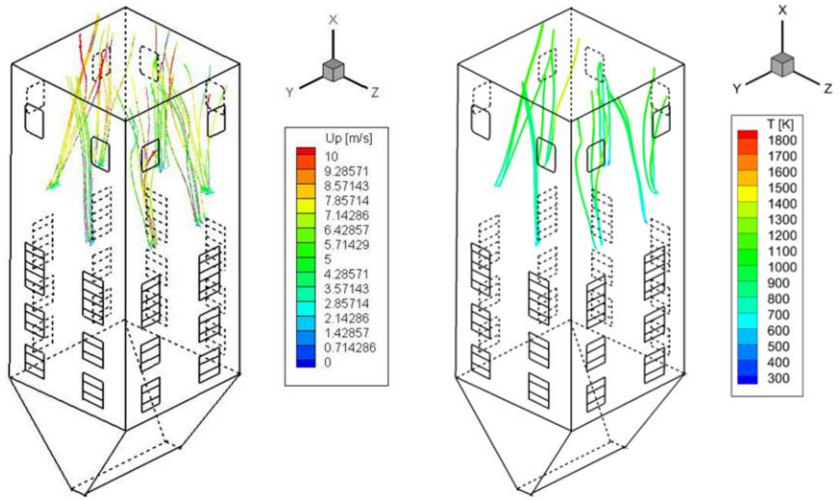

a) b)

Figure 7

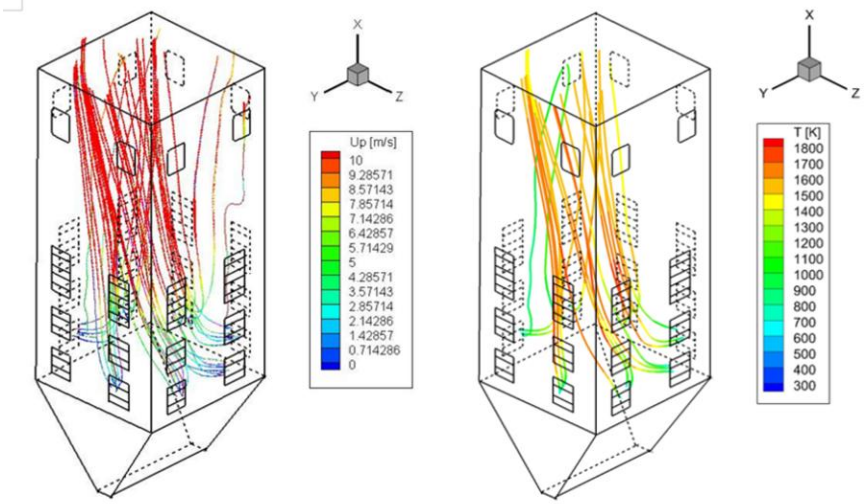

a) b)

Figure 8

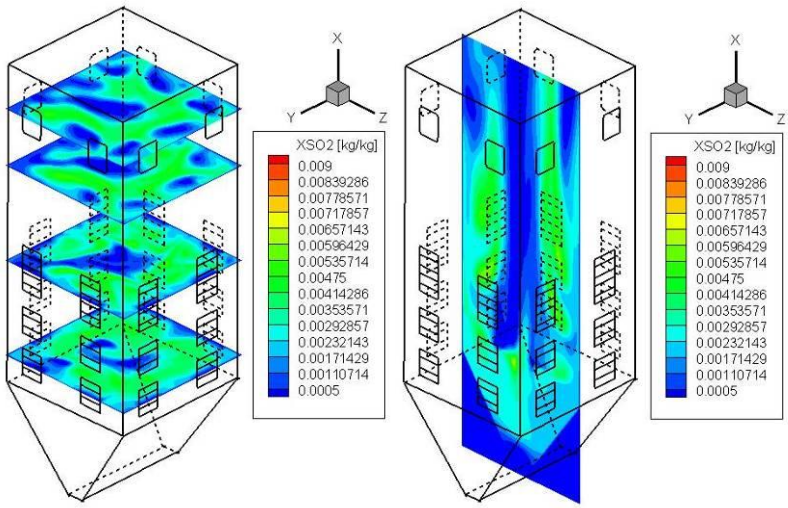

Figure 9

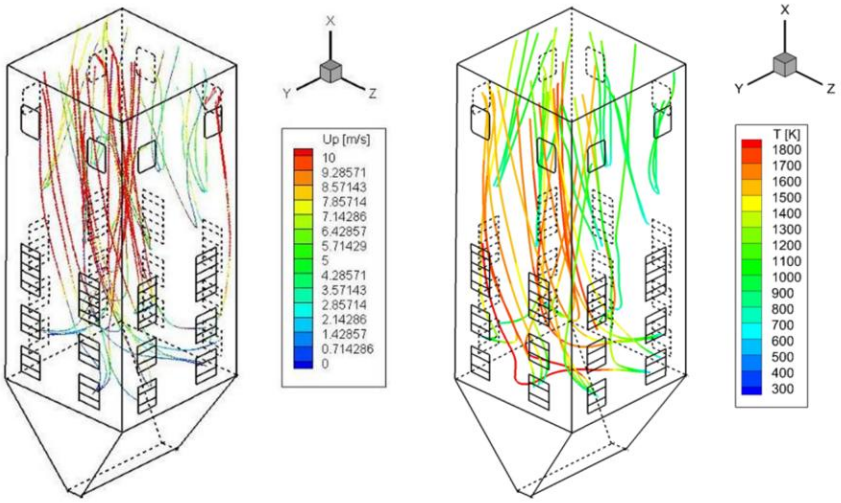

a) b)

Figure 10

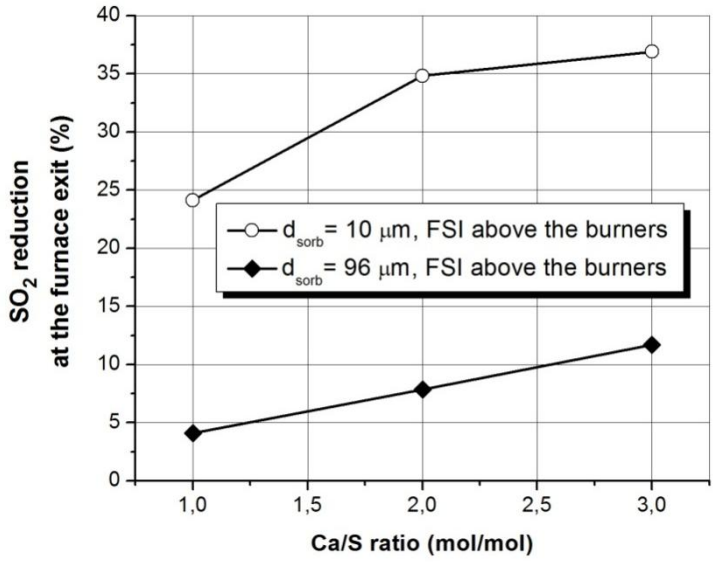

Figure 11

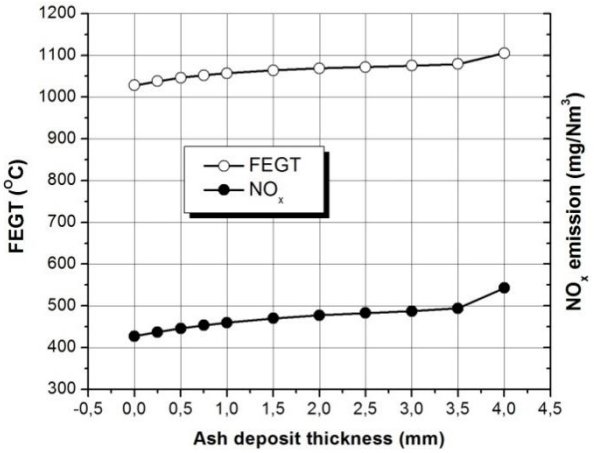

Figure 12

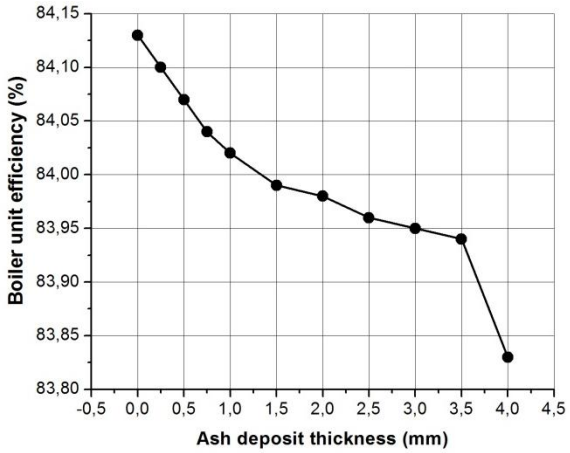

Figure 13

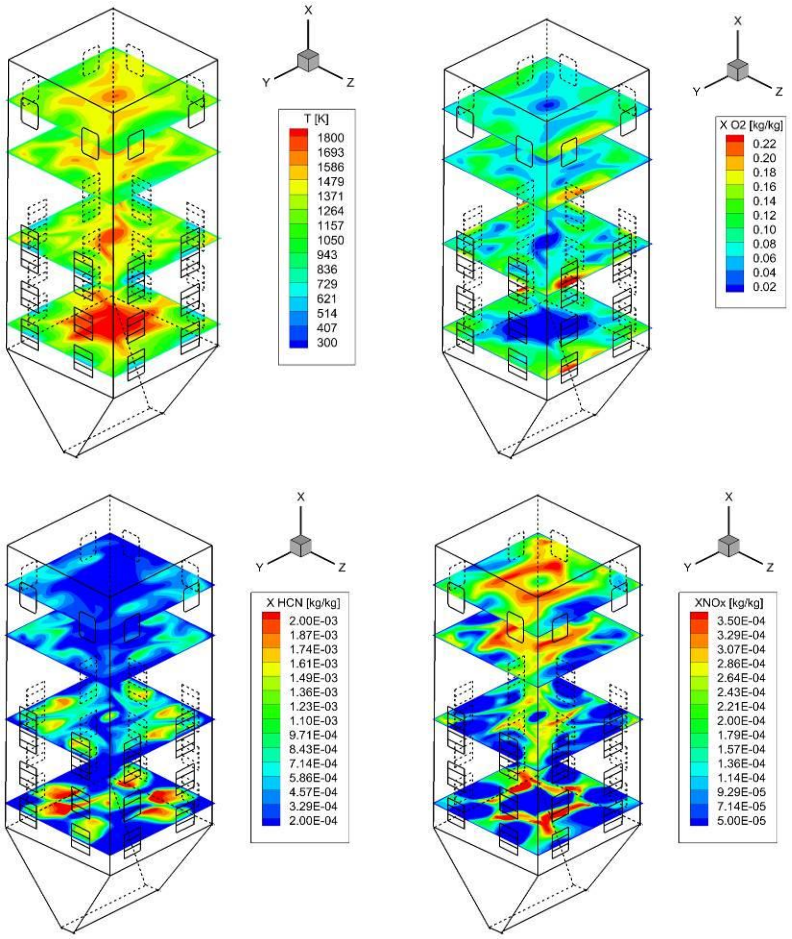

Figure 14

Table 1: NO_x/SO_2 emissions in FSI conditions for different grinding fineness of coal

Test-case	Initial coal particle size d_p (μm)	FEGT (°C)	NO_x emission, (mg/Nm^3)	SO^2 at the furnace exit (mg/Nm^3)/ SO_2 reduction (%)
TC1	150	1029	426.8	6816
TC1-FSI	150	1011	431.4	4359/36.0
TC1-100	100	1021	424.4	6791
TC1-100-FSI	100	1005	426.6	3922/42.2
TC1-50	50	994	435.7	6748
TC1-50-FSI	50	993	414.6	3567/47.1

Table 2: SO_2 reduction by FSI, NO_x and FEGT for different boiler loads

	Full load - 100 %			Partial load - 90 %		
Test-case	FEGT (°C)	NO_x/SO_2 content at furnace exit (mg/Nm^3)	SO_2 reduction at furnace exit (%)	FEGT (°C)	NO_x/SO_2 content at furnace exit (mg/Nm^3)	SO_2 reduction at furnace exit (%)
TC3	1092	464.1/6914	-	1085	481.5/6908	-
TC3-FSI	1066	440.1/5092	26.4	1059	455.5/5068	26.6
TC10	1069	424.5/6848	-	1062	431.8/6847	-
TC10-FSI	1048	416.2/4776	30.2	1043	424.6/4701	31.3
	Partial load - 80 %			[a]Partial load - 70 %		
Test-case	FEGT (^OC)	NO_x/SO_2 content at furnace exit (mg/Nm^3)	SO_2 reduction at furnace exit (%)	FEGT (^OC)	NO_x/SO_2 content at furnace exit (mg/Nm^3)	SO_2 reduction at furnace exit (%)
TC3	1075	501.6/6903	-	1045	496.8/6884	-
TC3-FSI	1050	476/4957	28.2	1023	480.0/5518	19.9
TC10	1053	437.6/6844	-	1024	440.5/6839	-
TC10-FSI	1036	430.7/4698	31.4	1004	438.4/5244	23.3

[a]six burners in operation (two burners turned off; for the rest of the cases seven burners in operation)

Table 3: FSI efficiency in the conditions of FGR for the Kostolac B boiler unit

Test-case	FEGT (°C)	Boiler exit gas temp. (°C)	Boiler efficiency coefficient (%)	NOx emission (mg/Nm3)	SO2 content (mg/Nm3) & SO2 reduction, at furnace exit (%)
[a]**TC8463** ([b]VFGR = 4.9%)	1047	171	85.79	564.2	5605
[a]TC8463-FSI (VFGR = 4.9%)	1039			536.4	3426 & 38.9
TC8463-7 ([c]RI & VFGR = 0%)	1087	160	86.56	748.0	6060
TC8463-7-FSI (RI &VFGR = 0%)	1063			677.6	3778 & 37.7
TC8463-8 (RI & VFGR=4%. NOx red. by FGR comp. to 8463-7: 14.1%)	1057	166	86.14	642.7	5802
TC8463-8-FSI (RI & VFGR = 4%)	1040			605.3	3702 & 36.2
TC8463-9 (RI & VFGR=8%. NOx red. by FGR comp. to 8463-7: 23.9%)	1028	172	85.74	569.1	5571
TC8463-9-FSI (RI & VFGR = 8%)	1018			531.9	3634 & 34.8
[a]**TC8226** (VFGR = 4.9%)	1041	171	85.63	541.6	5762
[a]TC8226-FSI (VFGR = 4.9%)	1028			536.2	3634 & 36.9

[a]seven mills in operation (in the rest of the cases six); [b]VFGR is flue gas recirculation (4.9%, as in nominal regime); [c]RI is reduced cold air ingress (13% into the furnace, as in nominal regime; in other test-cases 20%)